Diffusion-controlled reaction rate to a buried active site[a)]

René Samson and J. M. Deutch

Department of Chemistry, Massachusetts Institute of Technology, Cambridge, Massachusetts 02139
(Received 3 August 1977)

An approximate expression is presented for the rate coefficient k to an embedded active site. The site is located at a depth (sR) in a hollow channel whose sides are located at the polar angle θ_0, in a sphere of radius R. The result is $k(\theta_0,s)=(2\pi DR)[1-\cos\theta_0][(1-s)/s+\eta(\cos\theta_0)]^{-1}$, where D is the diffusion coefficient and $\eta(x)$ is given as a series of Legendre polynomials.

I. INTRODUCTION AND SUMMARY OF RESULTS

It is well known that in many enzymes the active site where the attachment of the substrate takes place is tucked inside of the enzyme.[1] In order to reach the active site, the substrate molecule must diffuse into the structure in the inert region of the enzyme. The usual theoretical studies of enzyme kinetics do not consider the complications arising from this fact.

In the simple theory due to Smoluchowski,[2] the enzyme is modelled as a sphere with its reactivity homogeneously distributed over the surface. Somewhat more realistically, Alberty and Hammes,[3] Solc and Stockmayer,[4] and Kuo-Chen and Shou-Ping[5] have considered a spherical geometry where only part of the surface is reactive (see Fig. 1). Here we consider a somewhat more complicated situation where the active site is a small spherical cap buried inside an inert sphere (Fig. 2). We seek an estimate of the difference in reaction rates for the two models (Figs. 1 and 2) in order to obtain an impression of the effect of an active site which is buried in the interior of the enzyme.

The model assumes the diffusion of pointlike "substrate molecules" to the active site in the enzyme to be the rate-determining factor. Accordingly, our purpose here is to isolate a single effect; the burying of the site. Complications arising from the molecular structure of the substrate, substrate-enzyme potential forces (whether electrostatic or van der Waals),[5,6] hydrodynamic interactions,[7] and dynamical conformational changes of the enzyme[8] are all ignored. Each one of these factors may have a major effect on the observed rate. Thus the analysis is restricted to circumstances where the overall rate of reaction is diffusion controlled. In addition, we neglect the effect of overall rotation of the target particle. The influence of rotation has been investigated by Solc and Stockmayer[4] for the case of a surface site; if the characteristic rotational diffusion time is comparable to or smaller than the characteristic time for reaction, one expects larger rates and weaker dependence on site geometry than obtained here.

The salient results of our investigation for the diffusion-controlled rate to a buried reactive site are contained in the approximate formula

$$k(\theta_0,s)/[4\pi DR]=\frac{1}{2}\,[1-\cos\theta_0]\left[\left(\frac{1-s}{s}\right)+\eta(\cos\theta_0)\right]^{-1}, \tag{1.1}$$

where D is the diffusion coefficient of the substrate molecules, R is the radius of the target enzyme, θ_0 is the polar angle presented by the buried site that lies at a radius (sR) within the enzyme (see Fig. 2). The function $\eta(\cos\theta_0)$ is

$$\eta(x)=\frac{1}{2}\left[(1-x)+\sum_{l=1}^{\infty}\frac{P_{l-1}(x)-P_{l+1}(x)}{l+1}\right]. \tag{1.2}$$

We note that this approximate formula has the following sensible limiting behavior: (1) When $\theta_0\to\pi$ one has a uniformly reactive sphere of radius $\rho=sR$; since $\eta(-1)=1$, Eq. (1.1) predicts $k(\theta_0=\pi,\,s)=4\pi D\rho$ as expected.[2] (2) When $\theta_0\to 0$ one has no active site and $k(0,\,s)=0$ as required. (3) For $s=1$ one has the case of a surface active site for $0<\theta<\theta_0$ and the predicted behavior for the reaction rate is

$$k(\theta_0,\,1)/[4\pi DR]=\tfrac{1}{2}[1-\cos\theta_0]/\eta(\cos\theta_0). \tag{1.3}$$

This case closely resembles a limiting case (no rotation) considered by Solc and Stockmayer,[4] who obtain, however, in place of $\eta(\cos\theta_0)$ the function $\eta'(\cos\theta_0)$

$$\eta'(x)=\frac{1}{2}(1-x)+\frac{1}{4}\,\frac{1}{(1-x)}\sum_{l=1}^{\infty}\frac{[P_{l-1}(x)-P_{l+1}(x)]^2}{(l+1)(l+\frac{1}{2})} \tag{1.4}$$

as an approximation to their numerical results. Fortunately, the numerical difference between employing either η or η' in Eq. (1.3) is insignificant.

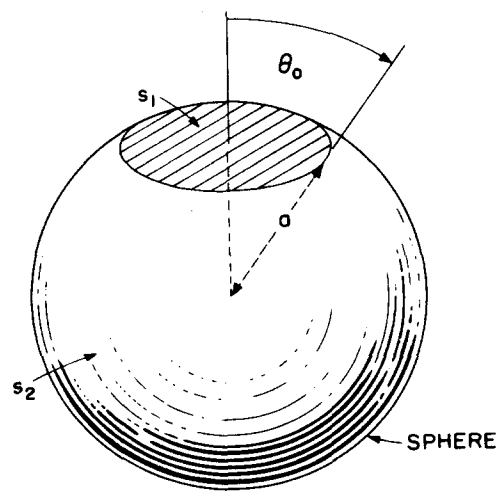

FIG. 1. Model I: simple sphere of radius a. The spherical cap S_1 is the active site, S_2 is the inert region of the enzyme surface. There is azimuthal symmetry around the vertical axis.

a)Supported in part by the National Science Foundation.

 0021-9606/78/6801-0285$01.00

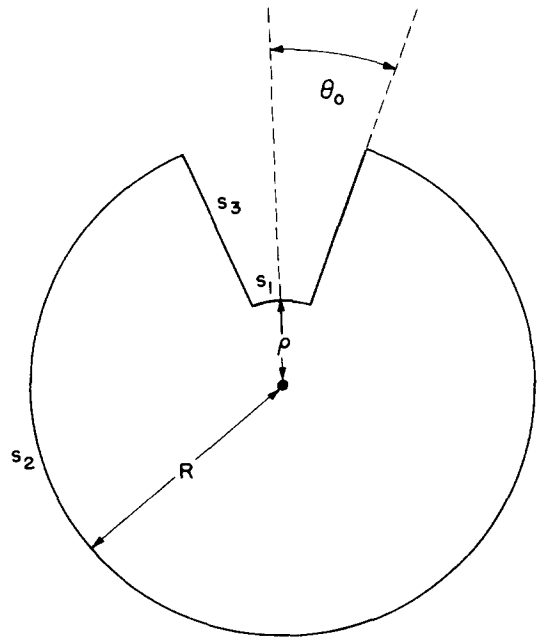

FIG. 2. Model II: in a sphere S_2 of radius R a conical duct S_3 is drilled which terminates in a spherical cap S_1 of radius ρ. S_1 is the active site, S_2 and S_3 are inert. There is azimuthal symmetry around the vertical axis. θ_0 is the openings angle of the conical duct. By definition, $s=\rho/R$.

In summary, we propose that Eq. (1.1) can be employed to estimate the diffusion-controlled rate of substrate molecules to a buried site in a larger target molecule. Since the model is idealized to contain only the effects of diffusion and many complications (such as those mentioned above) are not included, the expression for $k(\theta_0, s)$ should be applied to real enzymatic systems with caution.

The remainder of this article is devoted to a presentation of the approximate analysis that led to Eq. (1.1) and illustrative results for $k(\theta_0, s)$ as a function of θ_0 and s.

II. SPECIFICATION OF THE MODEL

We solve the steady-state diffusion equation for the local concentration $\phi(\mathbf{r})$ of substrate particles

$$\nabla^2\phi(\mathbf{r})=0, \tag{2.1}$$

subject to the following boundary conditions

$$\phi\to\phi_0 \text{ when } r\to\infty \tag{2.2}$$

$$\phi(\mathbf{r})=0 \text{ at the active site} \tag{2.3}$$

$$\frac{\partial\phi(\mathbf{r})}{\partial\eta}=0 \text{ at the inert surface region of the enzyme} \tag{2.4}$$

(here, $\partial/\partial\eta$ denotes the normal derivative). In Secs. II.A and III this boundary-value problem is solved for the two models of Figs. 1 and 2 (to be referred to as models I and II henceforth). Comparison of the results shows that the rate in model II is substantially less than that in model I when the angle θ_0 is small.

A. Sphere with external active patch (model I)

The Laplace equation (2.1) can be rewritten in terms of an integral equation[9] for ϕ with the boundary conditions (2.2)–(2.4) automatically satisfied

$$\phi(\mathbf{r})=\phi_0-\frac{1}{4\pi}\int_{S_1}d\mathbf{r}'\,\frac{1}{|\mathbf{r}-\mathbf{r}'|}\,\frac{\partial\phi}{\partial r'} + \frac{1}{4\pi}\int_{S_2}d\mathbf{r}'\,\phi(\mathbf{r}')\frac{\partial}{\partial r'}\,\frac{1}{|\mathbf{r}-\mathbf{r}'|}. \tag{2.5}$$

This is solved by the following series of Legendre polynomials $P_l(x)$

$$\phi(r,\theta)=\phi_0\left[1-\sum_{l=0}^{\infty}f_l(\theta_0)\left(\frac{a}{r}\right)^{l+1}P_l(\cos\theta)\right], \tag{2.6}$$

where the expansion coefficients f_l satisfy the following set of linear equations

$$\sum_{k=0}^{\infty}A_{lk}f_k=\tfrac{1}{2}l\alpha_{l0}(\theta_0), \qquad (l=0,1,2,\ldots). \tag{2.7}$$

Here,

$$A_{lk}=\frac{l+1}{2l+1}\delta_{lk}+\tfrac{1}{2}(l-k-1)\,\alpha_{lk}(\theta_0), \tag{2.8}$$

and

$$\alpha_{lk}(\theta_0)=\int_{\cos\theta_0}^{1}dx\,P_l(x)P_k(x). \tag{2.9}$$

It is readily verified that when $\theta_0=\pi$, $f_l=0$ for $l\geq 1$, as required. Generally, Eq. (2.7) can be solved numerically. In the numerical solution one must impose an upper limit on the dimension of the system $N\geq l, k$. It is not clear *a priori* whether the calculated $\phi_N(\mathbf{r})$ converges smoothly to the correct result when $N\to\infty$ and how large N must be to satisfy a certain convergence criterion. We presently return to this problem.

The reaction rate k is proportional to the integrated flux of diffusing particles over a surface σ enclosing the sphere

$$k\equiv\frac{D}{\phi_0}\int_{\sigma}d\mathbf{r}\,\frac{\partial\phi}{\partial\eta}. \tag{2.10}$$

According to Gauss' theorem this integral is the same for *any* surface σ enclosing the reaction surface. If σ is chosen to be a spherical surface with radius $R>a$, then one finds

$$k=4\pi D a\,f_0(\theta_0). \tag{2.11}$$

In Fig. 3, the reduced reaction rate $k^*\equiv k/4\pi Da=f_0$ is plotted as a function of θ_0. The crosses and circles pertain to two different values for the Legendre cutoff parameter N; namely, $N=10$ and 30, respectively. It is seen that as $\theta_0\to\pi$, k approaches the well known Smoluchowski result $4\pi Da$.

At not too small angles (say, $\theta_0\geq\pi/10$) the variation of k^* with N (in the range of 10–30) is not large (less than 20%), indicating that the algorithm is reasonably stable, although the possibility cannot be excluded that for much higher values of N the results would change appreciably. However, at smaller angles one observes increasing numerical instability. For example, at θ_0

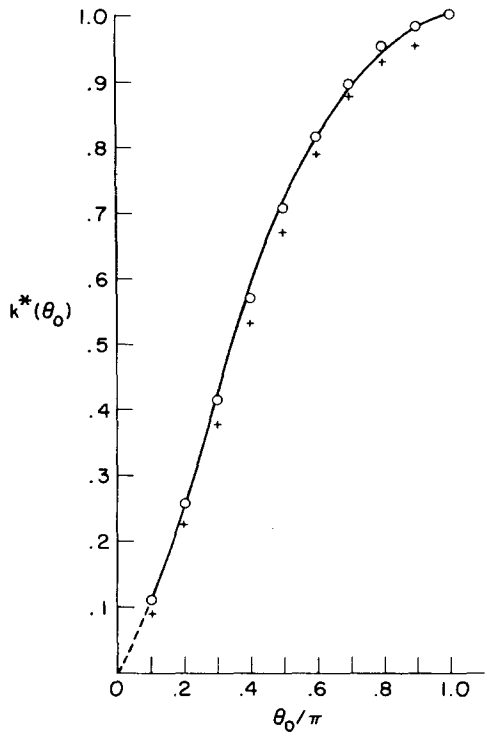

FIG. 3. The reduced rate k^* as a function of θ_0 for model I. The circles pertain to calculations with $N=30$, the crosses are for $N=10$. At small angles (dotted part of the curve) there is a large uncertainty in the computed numbers.

$=\pi/100$, $f_0(\theta_0)$ for $N=10$ and $N=30$ differ by a factor of 14. The occurrence of this instability is not surprising; at the surface of the enzyme the function $\phi(a, \theta)$ and its normal derivative change sharply in the region around $\theta=\theta_0$. In order to represent this accurately with a Legendre series, one needs a very large number of terms.

For small angles θ_0 a different approximation method is obviously required. The well known sum rule for Legendre polynomials

$$\sum_{l=0}^{\infty}(l+\tfrac{1}{2})P_l(x)P_l(x')=\delta(x-x')\,, \tag{2.12}$$

makes it a simple matter to construct functions of θ that vanish on a given interval and are finite elsewhere. For example, a function that satisfies the condition that $\partial\phi/\partial r\,(a, \theta)=0$ for $\theta>\theta_0$ is

$$\phi(r, \theta)=\phi_0\left[1-\frac{1}{\eta}\sum_{l=0}^{\infty}\frac{l+\frac{1}{2}}{l+1}\alpha_{l0}(\theta_0)\left(\frac{a}{r}\right)^{l+1}P_l(\cos\theta)\right], \tag{2.13}$$

where η is as yet undetermined and $\alpha_{l0}(\theta_0)$ is defined in Eq. (2.9). Instead of attempting to find an exact solution which would satisfy $\phi(a, \theta)=0$ for $\theta<\theta_0$, an approximate solution is obtained by requiring $\phi(a, \theta)$ to vanish only at $\theta=0$ (i.e., at the center of the active site). This implies that

$$\eta(\theta_0)=\sum_{l=0}^{\infty}\frac{l+\frac{1}{2}}{l+1}\alpha_{l0}(\theta_0)=\frac{1}{2}\left((1-\cos\theta_0)+\sum_{l=1}^{\infty}\frac{P_{l-1}(\cos\theta_0)-P_{l+1}(\cos\theta_0)}{l+1}\right). \tag{2.14}$$

It can be shown that this sum is rapidly convergent.

From Eqs. (2.6), (2.11) and (2.13) we obtain

$$k^*\equiv\frac{k}{4\pi Da}=\frac{1}{2}\frac{(1-\cos\theta_0)}{\eta(\theta_0)}\,. \tag{2.15}$$

One finds numerically that $\phi(a, \theta)$, when averaged over the patch, differs very little from zero, thus supporting the approximation that determines η only from the condition $\phi(a, \theta=0)=0$. An estimate of the error introduced by this approximation is provided by the quantity $\epsilon(\theta_0)$, which is defined as

$$\epsilon(\theta_0)=\frac{1}{\mathfrak{N}}\int_{\cos\theta_0}^{1}d\cos\theta\phi(a, \theta), \tag{2.16}$$

where for the normalization constant $\mathfrak{N}$ we arbitrarily take the integrated flux

$$\mathfrak{N}(\theta_0)=a\int_{\cos\theta_0}^{1}d\cos\theta\left(\frac{\partial\phi(r, \theta)}{\partial r}\right)_{r=a}. \tag{2.17}$$

The quantity $\epsilon(\theta_0)$ varies almost linearly from zero to 0.04 in the range $\theta_0=0$ to $\theta_0=\pi/10$.

In Figs. 4 and 5 we present respectively results for $\eta(\theta_0)$ and $k^*(\theta_0)$ for $\theta_0\leq\pi/10$.

The small-angle approximation Eq. (2.15) has the additional desirable feature of smoothly joining the large-angle numerical results in the vicinity of $\theta_0=\pi/10$. Moreover, the small-angle approximate result approaches

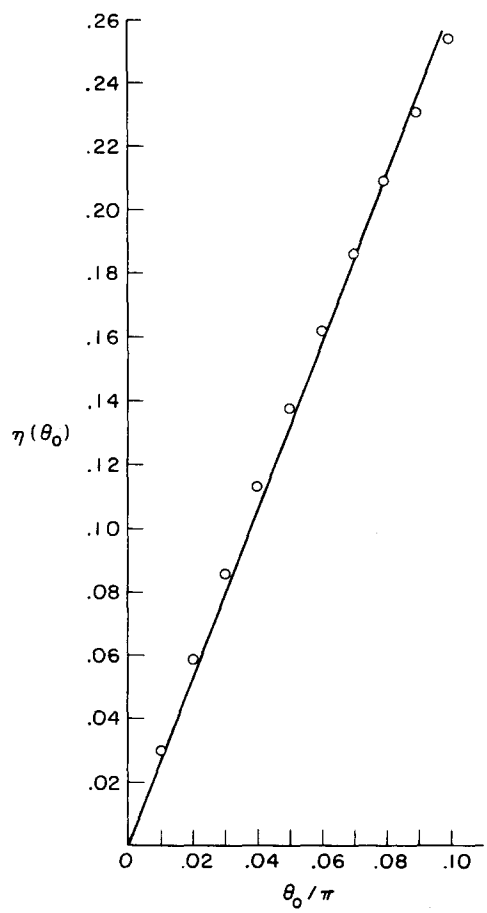

FIG. 4. Plot of the function $\eta(\theta_0)$ defined in Eq. (2.14) for $\theta_0\leq\pi/10$. Circles are calculated numbers, line is the best linear fit.

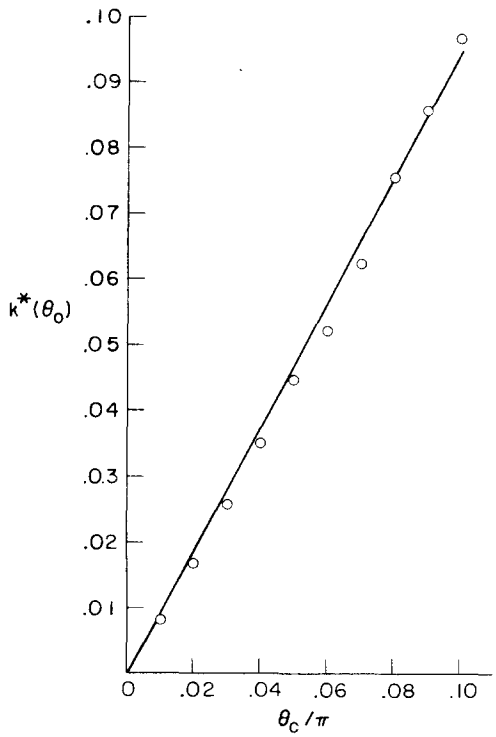

FIG. 5. The reduced reaction rate k^* as a function of θ_0 for model I for small angles ($\theta_0 \leq \pi/10$). Circles are calculated numbers, line is the best linear fit.

the correct limiting value $k^* = 1$ at $\theta_0 = \pi$. Accordingly, we may employ the small-angle approximation throughout the entire range $0 \leq \theta_0 \leq \pi$ without appreciable error. In Fig. 6 the predicted values for k^* vs θ_0 are plotted for both the numerical approximation and the small-angle approximation Eq. (2.15) in the region $\pi/10 \leq \theta_0 \leq \pi$. It can be seen that the approximation Eq. (2.15) differs from the correct numerical result by less than 20% throughout this region.

At small angles, k^* is approximately a linear function of θ_0. This might be expected on the basis of the Smoluchowski law $k = 4\pi Da$, which shows that k is proportional to the square root of the surface area for a homogeneous sphere.

The linear dependence of k^* on θ_0, i.e., $(\text{area})^{1/2}$ for small θ_0, could be a consequence of the simplification in the boundary condition that requires $\phi(a, \theta)$ to vanish only at $\theta = 0$. The possibility of a quadratic dependence of k^* on θ_0, i.e., (area) for small θ_0 when the exact boundary condition is asserted cannot be excluded. Indeed, one knows from the work of Solc and Stockmayer[4] for the case of "chemical" boundary conditions where the combination $[\phi + \gamma(\partial\phi/\partial r)]$ is required to vanish on the reactive patch, that k^* is a linear function of area for small θ_0 as expected. There may, however, be a subtle change in functional dependence of k^* on θ_0, for small θ_0, as $\gamma \to 0$, the pure diffusion-controlled case.

III. CASE WHERE THE ACTIVE SITE IS INSIDE (MODEL II)

The sum rule (2.12) may also be employed to construct a more general class of functions which have a vanishing normal derivative at S_2. For the "outside" solution ($r \geq R$) the following function has the correct behavior at S_2 (see Fig. 2)

$$\phi_{\text{out}}(r, \theta) = \phi_0\left[1 - \sum_{l=0}^{\infty}\sum_{k=0}^{\infty} c_k \alpha_{kl}(\theta_0)\frac{l+\frac{1}{2}}{l+1}\left(\frac{R}{r}\right)^{l+1} P_l(\cos\theta)\right], \tag{3.1}$$

where the c_k are as yet undetermined. We expand the "inside" solution ($\rho \leq r \leq R$, $0 \leq \theta \leq \theta_0$) in terms of the Legendre polynomials $P_l(\cos\pi\theta/\theta_0)$ which form a complete set on the interval $[0, \theta_0]$. Furthermore, they satisfy

$$\frac{\partial}{\partial\theta} P_l\left(\cos\frac{\pi\theta}{\theta_0}\right)\Big|_{\theta=\theta_0} = 0, \tag{3.2}$$

so that the boundary condition at S_3 is automatically obeyed. If we choose

$$\phi_{\text{in}}(r, \theta) = \phi_0 \sum_{l=0}^{\infty} b_l\left[\left(\frac{r}{\rho}\right)^l - \left(\frac{\rho}{r}\right)^{l+1}\right] P_l\left(\cos\frac{\pi\theta}{\theta_0}\right), \tag{3.3}$$

then the boundary condition at S_1 is also satisfied. The unknown coefficients b_l and c_l can now be fixed by the continuity conditions on ϕ and $\partial\phi/\partial r$ across the opening of the tunnel. This gives rise to a set of coupled linear equations for the b_l and the c_l which can be solved numerically. Again, a cutoff parameter $N \geq l$, k must be imposed. The resulting solution for the reaction rate is found to be violently unstable against variations in N for all values of the parameters θ_0 and $s \equiv \rho/R$.

In order to make progress we must again resort to approximation procedures. In analogy to Sec. II, we shall use an approximation which is expected to give good re-

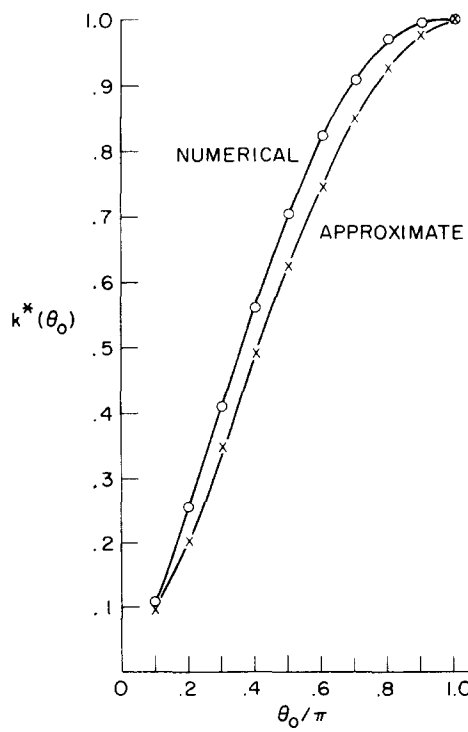

FIG. 6. The reduced reaction rate k^* as a function of θ_0 for model I: comparison between "numerical" approximation (same as in Fig. 3) and the small-angle approximation (curve labeled approximate).

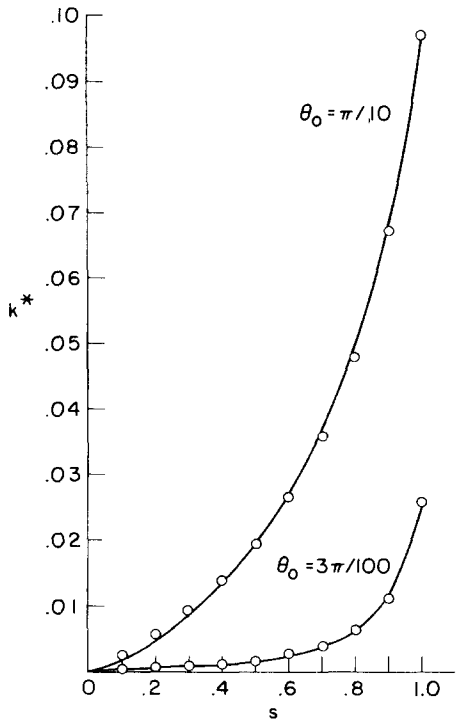

FIG. 7. The reduced reaction rate k^* as a function of the ratio of the radii $s = \rho/R$ for model II for angles $\theta_0 = \pi/10$ and $3\pi/100$. Note that at $s = 1$ the results for model I (see Fig. 5) are retrieved.

sults for small opening angles θ_0. For the outside solution we shall use instead of Eq. (3.1) the more restrictive function of Eq. (2.13)

$$\phi_{\text{out}}(r, \theta) = \phi_0\left[1 - \frac{1}{h}\sum_{l=0}^{\infty}\frac{l+\frac{1}{2}}{l+1}\alpha_{l0}(\theta_0)\left(\frac{R}{r}\right)^{l+1}P_l(\cos\theta)\right]. \quad (3.4)$$

In order to fix h and b_l ($l = 0, 1, 2, \ldots$) we shall impose the following conditions: (1) $\partial\phi/\partial r$ is continuous across the opening of the channel, and (2) $\phi_{\text{in}}(R, \theta = 0) = \phi_{\text{out}}(R, \theta = 0)$. From these conditions it follows that $b_l = 0$ for $l > 0$ (i.e., the gradient across the opening of the channel is independent of θ) and

$$h(s, \theta_0) = \frac{1-s}{s} + \eta(\theta_0), \quad (3.5)$$

where $s \equiv \rho/R$ ($0 \le s \le 1$) and $\eta(\theta_0)$ is given by Eq. (2.14). Condition (2) is an approximation since it requires continuity in ϕ only at the center of the opening rather than across the entire channel. A rough estimate of the error made as a result of this approximation can be obtained similarly as in Eq. (2.16) through the quantity ϵ. From Eq. (3.4) one obtains the reduced reaction rate

$$k^*(\theta_0, s) = \frac{k(\theta_0, s)}{4\pi DR} = \frac{1}{2}\,\frac{1-\cos\theta_0}{h(s, \theta_0)}. \quad (3.6)$$

Substitution of Eq. (3.5) into Eq. (3.6) leads to the principal result of our analysis, Eq. (1.1). Since $k^*(\theta_0, s)$ smoothly goes over to the external patch results (model I) as $s \to 1$, and gives the correct limiting

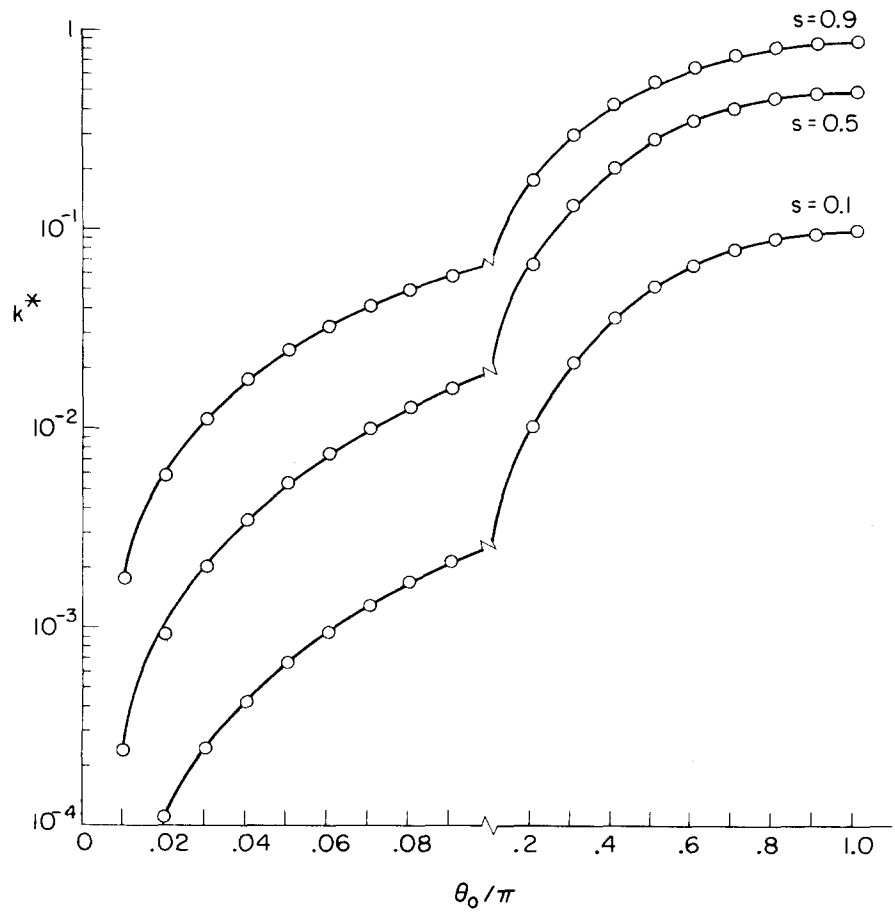

FIG. 8. The reduced reaction rate k^* as a function of θ_0 for $s = 0.1$, 0.5, and 0.9 (model II). Note the change in scale occurring at $\theta_0 = \pi/10$.

behavior $k^* = \rho$ as $\theta_0 \to \pi$, we propose to use Eq. (3.6) for all values of s and θ_0.

In Fig. 7, k^* is presented as a function of s for $\theta_0 = \pi/10$ and $3\pi/100$; Fig. 8 presents k^* as a function of θ_0 for $s = 0.1$, 0.5, and 0.9. Note that for $\theta_0 = \pi/10$, $s = \frac{1}{2}$, $k^*(\pi/10, \frac{1}{2}) = 0.0195$, and that for $\theta_0 = \pi/10$, $s = 1$, $k^*(\pi/10, 1) = 0.0968$. Thus as an illustrative case we find that the reduction in diffusion-controlled reaction rate from an active site buried halfway down a 36° channel is a factor of $0.20 = k^*(\pi/10, \frac{1}{2})/k^*(\pi/10, 1)$. This reduction should be compared to a factor of 0.5, which would be predicted on the basis of the change in the square root of the surface area presented when the site is buried to $s = \frac{1}{2}$. For a 10.8° channel, $k^*[(3\pi/100), \frac{1}{2}]/k^*[(3\pi/100), 1] = 0.08$. This fraction is significantly less than the corresponding reduction in the square root presented surface area of the active site.

Finally, we note that an alternative procedure for approximating diffusion-controlled rates could be based on use of a variational principle. However, in the present case construction of sample trial functions that satisfy the boundary conditions inside and outside the channel is not trivial and accordingly we have not pursued this possibility.

[1]R. E. Dickerson and I. Geis, *The Structure and Action of Proteins* (Benjamin, Menlo Park, CA, 1969).
[2]M. v. Smoluchowski, Phys. Z. 17, 557 (1916); Z. Phys. Chem. 92, 129 (1917).
[3]R. A. Alberty and G. G. Hammes, J. Phys. Chem. 62, 154 (1958).
[4]K. Solc and W. H. Stockmayer, J. Chem. Phys. 54, 2981 (1971); K. Solc and W. H. Stockmayer, Int. J. Chem. Kinet. 5, 733 (1973).
[5]C. Kuo-Chen and J. Shou-Ping, Sci. Sin. 17, 664 (1974).
[6]P. Debÿe, Trans. Electrochem. Soc. 82, 265 (1942).
[7]J. M. Deutch and B. U. Felderhof, J. Chem. Phys. 59, 1669 (1973) and references cited therein.
[8]J. A. McCammon and P. G. Wolynes, J. Chem. Phys. 66, 1452 (1977).
[9]J. D. Jackson, *Classical Electrodynamics*, 2nd ed. (Wiley, New York, 1975), p. 41.